Polar Meteorol. Glaciol., **16**, 61–73, 2002

A stratification model of surface snow at Dome Fuji Station, Antarctica

Yiying Zhou[1], Nobuhiko Azuma[1] and Takao Kameda[2]

[1] *Nagaoka University of Technology, 1603–1, Kamitomioka, Nagaoka 940-2188*
[2] *Kitami Institute of Technology, 165, Koencho, Kitami 090-8507*

Abstract: A stratification model of surface snow on the ice sheet, which includes snow density evolution, is proposed. Using the temperature profile in the surface snow layer obtained at Dome Fuji Station, Antarctica, snow density evolution under various accumulation conditions was simulated. It is demonstrated that water vapor diffusion is very important for the snow density evolution, and temperature and accumulation at the snow surface are the most important factors that determine the future snow density profile below the surface.

1. Introduction

It is considered that density and grain size of the surface snow of ice sheets reflect past climatic history. Recently, numerical models of snow stratigraphy, which simulate the evolution of density and grain size, have been proposed. Brun *et al.* (1989) developed a numerical model named "Crocus" to simulate snow temperature, liquid-water content and density profiles of snow layers using precipitation, air temperature, humidity, wind velocity, and incoming short-wave and long-wave radiation data. Brun *et al.* (1992) improved this model to simulate the evolution of snow-cover stratigraphy (*i.e.* the type and size of snow grains in each layer of the snow cover). Dang *et al.* (1997) examined Crocus's capability to reproduce the evolution of snow density and grain size of polar snow at the surface of an ice sheet, and found that the simulated snow density and grain size exhibit strong sensitivity to air temperature, accumulation rate and the initial density of deposited snow. However, the simulated snow temperature shows large errors compared to the observed data, which caused significant differences between the simulated density and grain size of snow and the observed ones. In order to avoid the influence of such quantities as air temperature and incoming radiation on the simulated snow temperature, in this study we use snow temperature data measured at Dome Fuji Station, Antarctica directly to simulate density variation in the surface snow layer.

The purpose of this paper is to make clear the effect of water vapor diffusion in the surface snow layer on the development of the snow layer stratification, and to investigate the cause and the mechanism of snow texture (*e.g.* grain size, grain shape and porosity) variation with depth in the surface snow layer in Antarctica. In the following sections, we describe the mechanisms of densification and water vapor diffusion in snow layers, and then present the formulae necessary to calculate the density and thickness changes

with time of each snow layer. In order to understand the separate effects of densification and water vapor diffusion in the process of layer stratification, we conducted several types of simulations with various accumulations in every month or in several months under the observed temperature condition. Finally, we compared the simulated results with field data obtained at Dome Fuji Station, Antarctica in 1995–1996.

2. Model

It is considered that vertical variations of snow density in the surface snow layers of an ice sheet are formed by densification due to overburden pressure and the transportation of mass due to water vapor diffusion in snow and the initial condition of snow deposited at the surface.

The strain rate of densification, $\dot{\varepsilon}$, of a snow layer is given by

$$\dot{\varepsilon} = -\frac{1}{h}\frac{dh}{dt} = \frac{1}{\rho}\frac{d\rho}{dt}, \tag{1}$$

where h is the thickness of a snow layer and ρ is the density of this layer. Here, the mass of each snow layer is assumed to be conserved, which means that it does not change by sublimation or condensation.

The strain rate ($\dot{\varepsilon}$) of snow is

$$\dot{\varepsilon} = \frac{d\varepsilon}{dt} = \frac{\sigma}{\eta}, \tag{2}$$

where ε is the strain, σ is the stress and η is the viscosity coefficient.

From eqs. (1) and (2), the compactive viscosity coefficient (η_c) can be expressed as

$$\eta_c = \sigma\rho \Big/ \frac{d\rho}{dt}, \tag{3}$$

where σ is the overburden pressure on a given snow layer and can be written as

$$\sigma = \sum_{i=1}^{n} \rho_i g h_i, \tag{4}$$

where h_i and ρ_i are thickness and density of the ith snow layer, respectively, and g is the gravity acceleration. According to Maeno and Kuroda (1986), the compactive viscosity coefficient of surface snow in Antarctica is given by:

$$\eta_c = (1.5\sim7.5)\times10^{-3}\exp(0.024\rho)\exp\left(\frac{Q}{RT}\right), \quad (\mathrm{Pa}\cdot\mathrm{s}) \tag{5}$$

where Q is the activation energy of snow densification, R is the gas constant and T is absolute temperature. From eqs. (3), (4), (5) and (1), the change of snow density with time due to overburden pressure $d(\rho_n)_d/dt$ and the change of snow thickness with time dh_n/dt can be written as

$$\frac{d(\rho_n)_d}{dt} = \frac{\rho_n \cdot \sum_{i=1}^{n} \rho_i g h_i}{(1.5\sim7.5)\times10^{-3}\exp(0.024\rho_n)\exp(\frac{Q}{RT})}, \tag{6}$$

$$\frac{dh_n}{dt} = -\frac{d(\rho_n)_d}{dt}\frac{h_n}{\rho_n}. \tag{7}$$

Now we consider the effect of water vapor diffusion. The vertical temperature gradient in snow causes the water vapor density gradient, so the water vapor diffuses from warmer snow with a higher vapor density to colder snow with a lower vapor density. The vapor flux (J) through a snow layer is given by

$$J = -D_{\text{eff}}\frac{\partial \rho_v}{\partial z} = -D_{\text{eff}}\left(\frac{\partial \rho_v}{\partial T}\right)_e \frac{\partial T}{\partial z}, \tag{8}$$

where D_{eff} is the effective vapor diffusion coefficient, ρ_v is vapor density, T is absolute temperature, z is depth and the subscript e denotes the phase-equilibrium condition. Since it has been found that the coefficient D_{eff} in snow is four to seven times larger than the diffusion coefficient in air (Yoshida, 1955; Colbeck, 1993), we define the effective vapor diffusion (D_{eff}) as

$$D_{\text{eff}} = 4 \times D = 4 \times 1.199 \times 10^{-9} T^{1.75}, \qquad (\text{m}^2\,\text{s}^{-1}) \tag{9}$$

where D is the vapor diffusion coefficient in air (Maeno and Ebinuma, 1983). Here we do not consider the dependence of D_{eff} on the density of snow.

According to Colbeck (1980), the vapor density (ρ_v) under the equilibrium condition varies with temperature and can be expressed as

$$\rho_v = p_0 \exp\left[\frac{L}{R}\left(\frac{1}{T_0} - \frac{1}{T}\right)\right] / RT, \tag{10}$$

where T_0 is the reference temperature, P_0 is the vapor pressure at T_0, L is the latent heat of sublimation at T_0 and R is the gas constant of water vapor. Applying eq. (10) to eq. (8) gives the water vapor flux equation

$$J = -D_{\text{eff}}\frac{p_0}{R^2}\frac{L - RT}{T^3}\exp\left[\frac{L}{R}\left(\frac{1}{T_0} - \frac{1}{T}\right)\right]\frac{\partial T}{\partial z}. \tag{11}$$

The conservation of mass gives

$$\left(\frac{\partial \rho}{\partial t}\right)_z + \left(\frac{\partial J}{\partial z}\right)_t = 0. \tag{12}$$

If we assume that the thickness of a snow layer does not change, neglecting densification due to overburden pressure, the density change of the snow layer is given by

$$\frac{d\rho_v}{dt} = -\frac{dJ}{dz} = \frac{d\left\{-D_{\text{eff}}\frac{P_0}{R^2}\frac{L - RT}{T^3}\exp\left[\frac{L}{R}\left(\frac{1}{T_0} - \frac{1}{T}\right)\right]\frac{\partial T}{\partial z}\right\}}{dz}. \tag{13}$$

So far we have explained the change of snow density caused by water vapor diffusion and densification separately. Now we combine both effects, water vapor diffusion and densification. The change of snow thickness is given by eq. (7). During a time increment Δt, a new snow layer is deposited on the snow surface, and hence, the nth snow layer becomes the $n+1$st snow layer after time Δt. The density of the snow

layer is given by

$$\rho_{n+1}(t+\Delta t)=\rho_n(t)+\mathrm{d}\rho_c, \tag{14}$$

$$\mathrm{d}\rho_c=\mathrm{d}(\rho_n(t)+\mathrm{d}\rho_v)_d, \tag{15}$$

where $\mathrm{d}\rho_c$ is the variation of snow density combining the effects of densification and water vapor diffusion during time increment Δt, $\mathrm{d}\rho_v$ is the variation of snow density due to water vapor diffusion during time increment Δt and subscript d denotes densification.

3. Simulation of snow density variation with depth

Using the 10 m deep snow temperature profile data (Azuma *et al.*, 1997) measured every hour in 1995–1996 at Dome Fuji Station, Antarctica, we conducted a simulation of the snow density evolution with depth under various accumulation conditions.

From the snow temperature data measured at time 0000 and time 1200 every day in 1995–1996, we calculated the average value of snow temperature in each month at the times 0000 and 1200 separately. Next, interpolated on the snow temperature with depth at intervals of 0.1 m, and then computed the density with depth in each month caused by water vapor diffusion and densification. The density of the surface snow is prescribed as 250 kg/m^3 here. For convenience, we used the average value of snow temperature in each month at time 0000 and 1200 in the simulation. Using the average snow temperature profile at the time 0000 the snow density change during a half month (that is, $\Delta t=15$ days), $\mathrm{d}\rho_c$ in eq. (15) was calculated, and then the snow temperature profile at the time 1200 was used for the other half month. We also calculated the snow density change every half-day using the snow temperature profiles at every midnight and every noon with the time increment of 12 hours. The difference of the simulated results for one year using both methods above is not significant. Therefore, we used the former method for several tens of years iteration. With regard to the input of snow accumulation, we set fresh snow on the surface at the beginning of each month.

Water vapor transport from the atmosphere to the surface snow should be calculated by the bulk method, which uses wind speed and the difference of saturated water vapor pressure on the snow surface and water vapor pressure at depth z. Because there are no wind speed or humidity data near the snow surface at Dome Fuji Station for 1995–1996, we assume that there is no wind, and water vapor is at saturation near the snow surface. Using the snow surface temperature and air temperature at depth 1.5 m, the water vapor diffusion balance on the snow surface is calculated. The boundary conditions on the surface are set as follows:

$$J=-D\frac{\partial\rho_v}{\partial z}=-D\left(\frac{\partial\rho_v}{\partial T}\right)_e\frac{\partial T}{\partial z}.$$

3.1. *The effect of densification*

First, using eqs. (6) and (7), the effect of densification due to overburden pressure on the change of each layer's thickness and density with depth after 10 years of repetition was examined.

3.1.1. Simulation A: Uniform accumulation

In order to examine the effect of accumulation rate on the density variation with depth, two cases were run, with accumulations of 10 mm and 5 mm of snow on the surface every month; 10 mm is comparable to the observed net accumulation at Dome Fuji Station.

The results in Fig. 1a show that in the case of 5 mm accumulation (thin line) the snow density increases with depth above 0.56 m more rapidly than that for 10 mm accumulation (thick line), and then the difference of density between two cases decreases with depth.

Without the effect of densification, the 10 years' accumulation becomes 0.6 m thickness in the case of 5 mm accumulation every month and 1.2 m thickness in the case of 10 mm accumulation every month, respectively. When considering the effect of densification, the surface snow of 10 years ago moves down to approximately 0.56 m depth and 1.08 m depth respectively for 5 mm accumulation and for 10 mm accumulation.

Figure 1b shows the time required to reach a given depth using the densification model in simulations A (1) and A (2) respectively. Because it takes much more time for a surface snow layer with a 5 mm accumulation model to reach the same depth in ten years than that with the 10 mm accumulation model, the density for the 5 mm accumulation model increases with depth more rapidly than that for the 10 mm accumulation model, as shown in Fig. 1a.

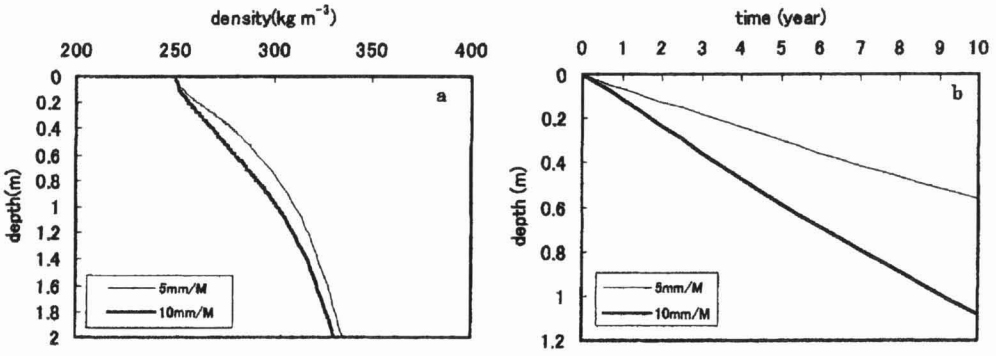

Fig. 1. (a) The result of simulation A: density-depth profiles for 10 mm/month accumulation (thick line) and for 5 mm/month accumulation (thin line) ($\eta_c = 1.5 \times 10^{-3}$exp (0.024ρ) exp (Q/RT)). (b) Depth-time relation using densification model for 10 mm/month accumulation (thick line) and for 5 mm/month accumulation (thin line).

3.1.2. Simulation B: Seasonal accumulation

In order to assess the effect of seasonal accumulation on the snow densification due to overburden pressure, simulation B was conducted for 2 cases: 1) 10 mm of snow accumulation on the surface was applied only in winter months (April, May, June, July, August, September). 2) 10 mm of snow accumulation on the surface was applied only in summer months (October, November, December, January, February, March).

Figure 2 shows the simulated density- depth profiles for winter accumulation

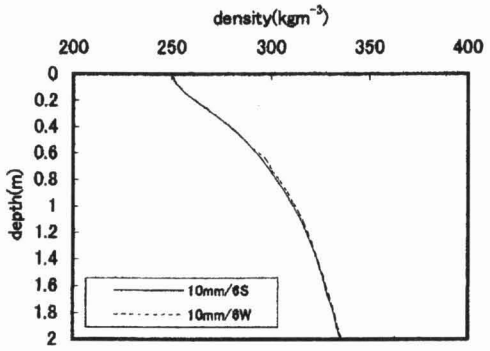

Fig. 2. The results of simulation B: density-depth profiles for winter accumulation (dashed line): 10 mm / month (April - September) + 0 mm / month (October - March) and for summer accumulation (solid line): 0/month (April-September) + 10mm/month (October-March) ($\eta_c = 1.5 \times 10^{-3} \exp(0.024\rho) \exp(Q/RT)$).

(dashed line) and for summer accumulation (solid line), which have no significant difference. If we assume that the initial accumulated snow density has no difference between winter and summer the effect of seasonal accumulation on the densification due to overburden pressure is negligibly small because the seasonal snow temperature difference in the surface snow layer does not significantly affect the snow densification.

3.2. The effect of water vapor diffusion

Figure 3 shows the water vapor flux variation with depth at intervals of 0.1 m at midnight (time 0000) and at noon (time 1200) in summer months (October, November, December, January, February, March) and winter months (April, May, June, July, August, September), respectively. Water vapor flux was calculated from the snow temperature profile data using eq. (11). It is evident that water vapor diffuses most actively in the uppermost 0.2 m, and it diffuses more actively in summer than in winter. Next, using eq. (13) that considers the effect of water vapor diffusion, the change of each layer's density was calculated for 10 years. In order to examine the effect of water vapor diffusion on the density variation with depth, two cases were run as described below.

3.2.1. Simulation C: Uniform accumulation

In order to assess the effect of accumulation rate on the density evolution due to water vapor diffusion, simulation C was run for 2 cases: 1) 10 mm of snow accumulation on the surface every month, 2) 5 mm of snow accumulation on the surface every month.

Figure 4 shows the results of simulation C: a) 10 mm snow accumulation and b) 5 mm snow accumulation. Both of the profiles show 10 cycles of low and high density alternation that may be considered annual layers. In Fig. 4b, density variation disappears below 0.6 m depth because the surface snow layer of 10 years ago does not reach below the depth of 0.6 m after 10 years of iteration, so that there are no data below 0.6 m. The profile in circle 2 that has little density change with depth corresponds to the winter layer (April-September), while the profile in circle 1 that has large density variation with depth corresponds to the summer layer (October-March). The large

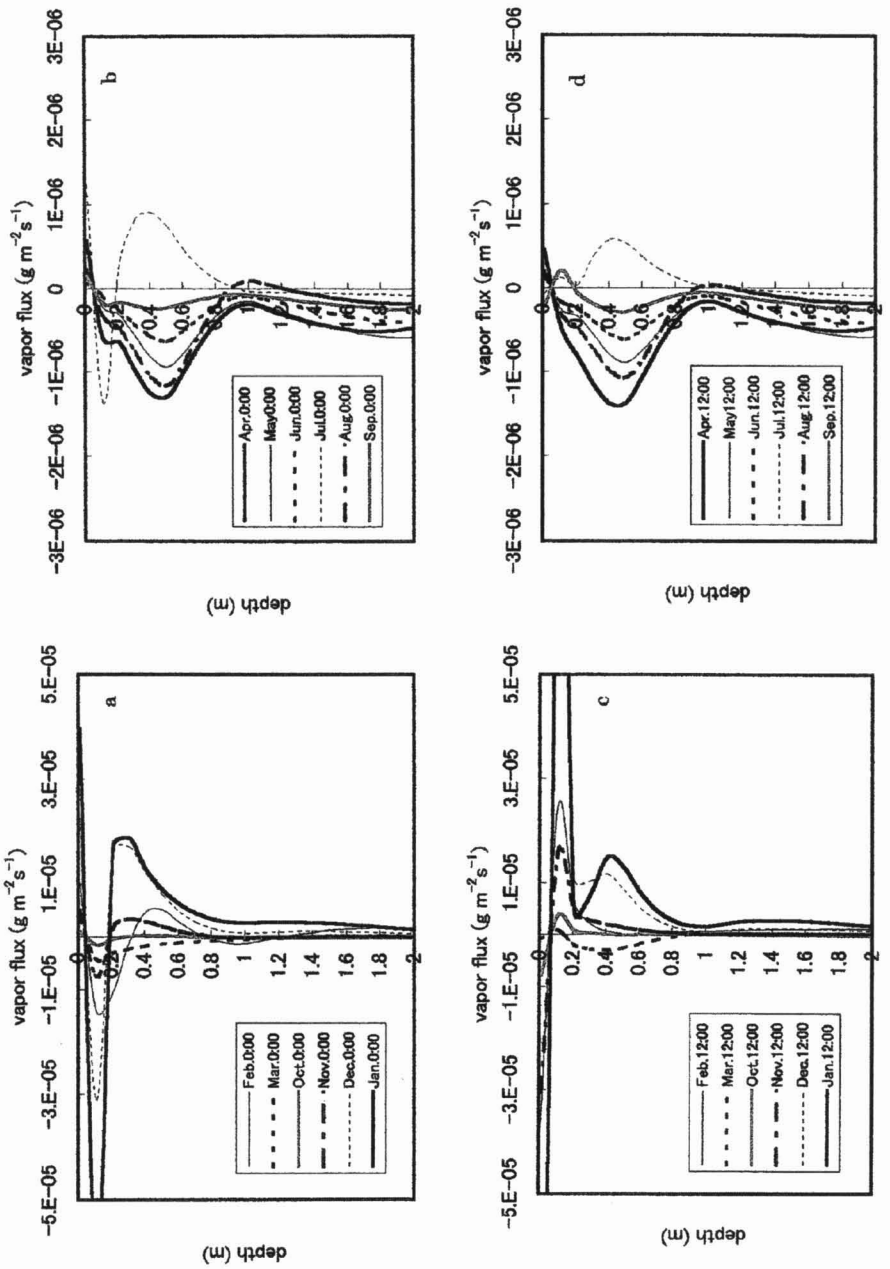

Fig. 3. Water vapor flux versus depth. (a) At midnight (time 0000) (October–March). (b) At midnight (time 0000) (April–September). (c) At noon (time 1200) (October–March). (d) At noon (time 1200) (April–September).

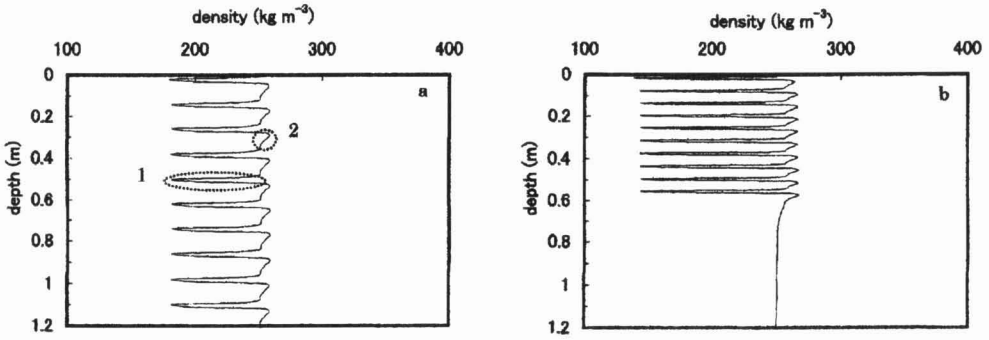

Fig. 4. The results of simulation C. (a) Density-depth profile for 10 mm/month accumulation. (b) Density-depth profile for 5 mm/month accumulation.

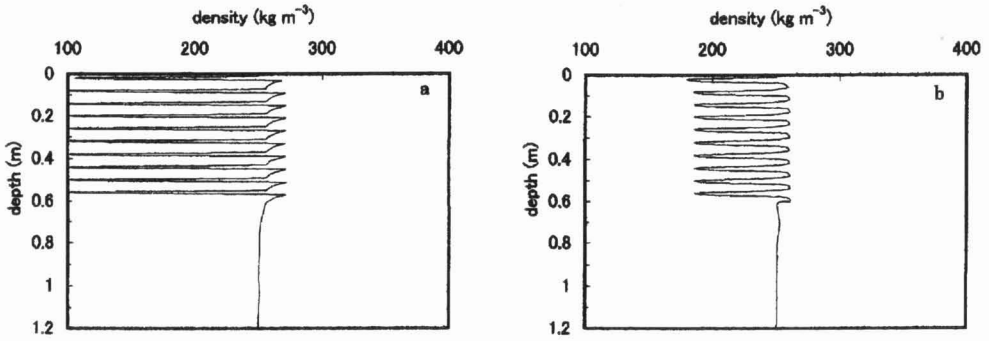

Fig. 5. The results of simulation D. (a) Density-depth profile for winter accumulation: 10 mm/month (April–September) + 0 mm/month (October–March). (b) Density-depth profile for summer accumulation: 0/month (April–September) + 10 mm/month (October–March).

gradient of water vapor flux near the surface results in a large density variation with depth, which is more remarkable in summer than in winter, as shown in Fig. 3. From this simulation we also found that the seasonal density variation is formed within the upper 50 cm of the surface snow layer and the water vapor flux gradient below the depth of 50 cm does not affect the seasonal density change profile significantly. Comparing with Fig. 4a and 4b, it is clear that a smaller accumulation rate results in a larger density variation with depth. This result is explained by the longer residence time near the surface for the accumulated snow with smaller accumulation rate.

3.2.2. Simulation D: Seasonal accumulation

In order to examine the effect of seasonal accumulation on the density variation due to water vapor diffusion, simulation D was run for two cases: 1) 10 mm of snow accumulation on the surface only in winter months (April, May, June, July, August, September), 2) 10 mm of snow accumulation on the surface only in summer months (October, November, December, January, February, March).

Figure 5 shows the results of simulation D that examined the effect of seasonal accumulation on the density evolution with depth. The density variation for only winter accumulation (Fig. 5a) is larger than that for only summer accumulation (Fig.

5b). In the surface snow layer, water vapor diffuses more actively in summer than in winter, so that the influence of water vapor diffusion on density evolution is larger in summer than in winter. In the case of winter accumulation the accumulated snow stays at the surface where water vapor diffusion is active during summer. Consequently, the density evolution becomes very large.

3.3. Combining the effects of densification and water vapor diffusion

Using eqs. (6), (7), (13), (14) and (15), we examined the total effect of densification due to overburden pressure and water vapor diffusion due to temperature gradient on the change of each layer's thickness and density with depth after 30 years iteration. The compactive viscosity coefficient of snow is taken as $1.5\times10^{-3}\exp(0.024\rho)\exp(Q/RT)$ (Pa·s) from eq. (5).

3.3.1. Simulation E: Uniform and seasonal accumulation

In order to assess the effect of uniform and seasonal accumulation on density variation due to both water vapor diffusion and overburden pressure, four cases were run: 1) 10 mm of snow accumulation on the surface every month, 2) 5 mm of snow accumulation on the surface every month, 3) 10 mm of snow accumulation on the surface only in winter months (April, May, June, July, August, September), 4) 10 mm

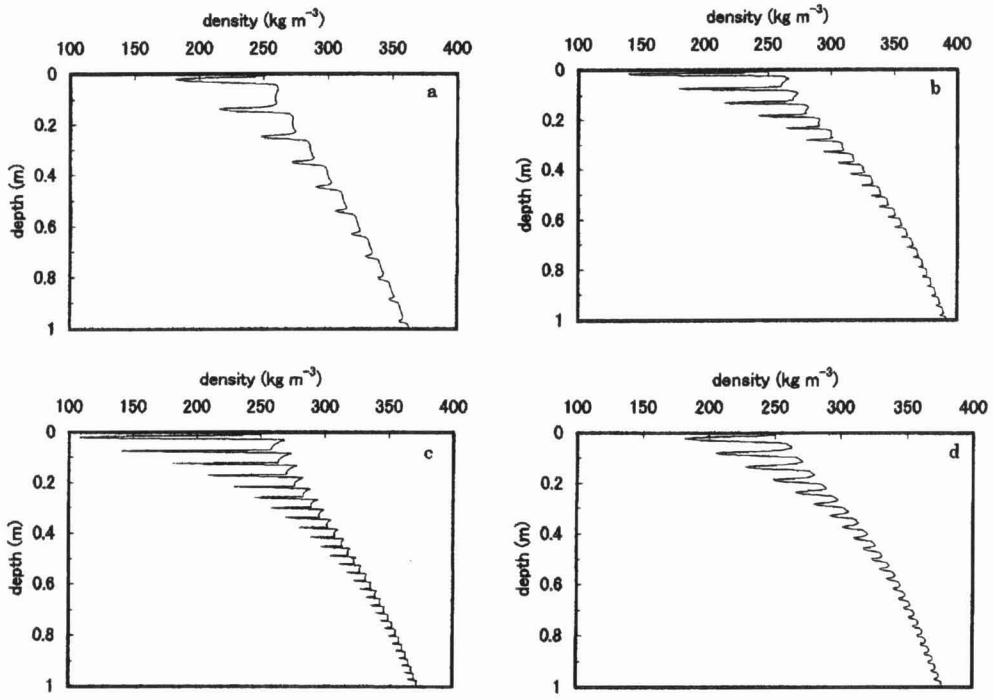

Fig. 6. The results of simulation E. (a) Density-depth profile for 10 mm/month accumulation. (b) Density-depth profile for 5 mm/month accumulation. (c) Density-depth profile for winter accumulation: 10 mm/month (April–September) + 0 mm/month (October–March). (d) Density-depth profile for summer accumulation: 0 mm/month (April–September) + 10 mm/month (October–March) ($\eta_c = 1.5\times10^{-3}\exp(0.024\rho)\exp(Q/RT)$).

of snow accumulation on the surface only in summer months (October, November, December, January, February, March).

Figure 6a, b, c and d show the results of simulations E(1), E(2), E(3) and E(4) respectively. It is clear from Fig. 6 that the variation of density in the annual layer decreases with depth due to snow densification and disappears within the upper one meter. However, this simulated result does not agree with the field observation that the annual layer identified by density variation is preserved down to the close-off depth or more. This discrepancy could be attributed to the large compactive viscosity of the depth-hoar layer. According to Kojima (1959), the experimental results on snow viscosity show that the depth-hoar layer has a much larger viscosity against gradual compaction than fine grained compact snow has. If we take the compactive viscosity coefficient of snow to be $7.5\times10^{-3}\exp(0.024\rho)\exp(Q/RT)$ (Pa·s) in the depth-hoar layers and $1.5\times10^{-3}\exp(0.024\rho)\exp(Q/RT)$ (Pa·s) in the other snow layers from eq. (5), we obtain the results of simulation E(1) and E(2) shown in Fig. 7.

Figure 7 shows that the seasonal variation of density is preserved with depth in spite of the effect of densification. This result agrees with observations in the field and by ice core analysis, that is, the low dense layer appears periodically with depth in snow stratigraphy. Therefore, we infer that the low dense layer composed of depth-hoar is more difficult to compress than other snow layers. This means that the compactive viscosity coefficient, eq. (5), should depend on not only density but also the shape of snow grains.

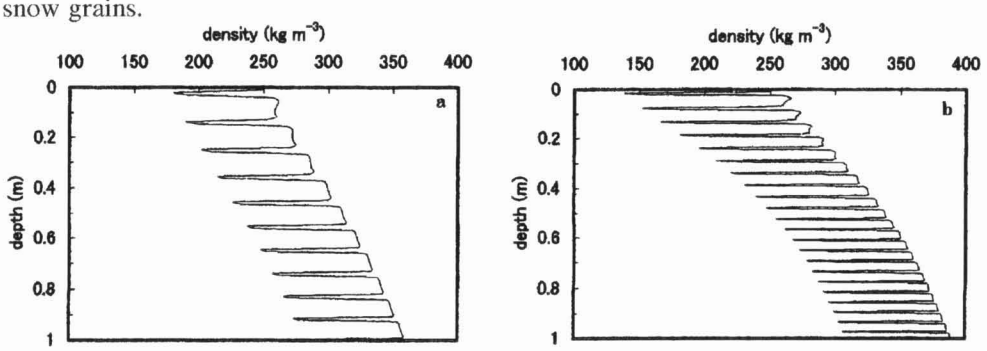

Fig. 7. The results of simulation E. (a) Density-depth profile for 10 mm/month accumulation. (b) Density-depth profile for 5 mm/month accumulation. ($\eta_c=7.5\times10^{-3}\exp(0.024\rho)\exp(Q/RT)$ in the depth-hoar layer and $\eta_c=1.5\times10^{-3}\exp(0.024\rho)\exp(Q/RT)$ in the other snow layers.)

3.3.2. Comparison of simulation results with field data

In order to compare the simulated results with the field data (Azuma *et al.*, 1997) measured in February, April, October and January of 1995–1996 at Dome Fuji Station, Antarctica, the simulation E(1) has been computed for 30 years iteration.

Figure 8 shows the simulated snow density considering the effects of densification and water vapor diffusion with the density data measured by pit study. Figure 9 shows the results using a large compactive viscosity coefficient for the depth-hoar layer. It is clear from Fig. 8 that the whole trend of simulated density agrees with that of measured data, which is considered to be mostly influenced by snow densification. Because the

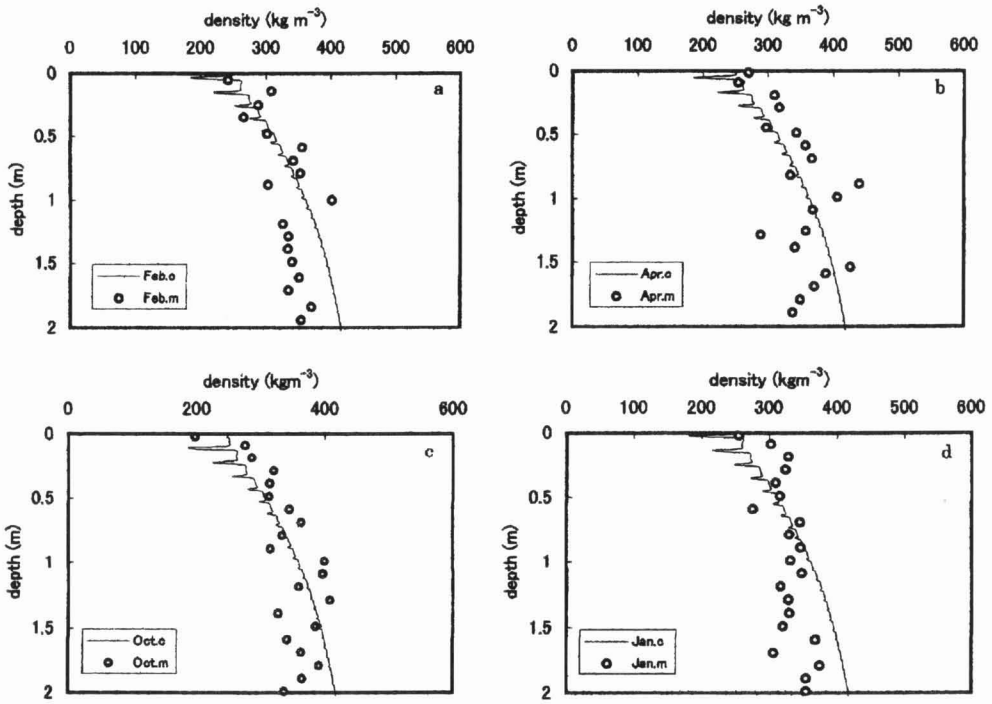

Fig. 8. Comparison of simulated (simulation E(1)) and measured snow density with depth. (a) February. (b) April. (c) October. (d) January. (Solid line is simulated density. Circle is measured density. $\eta_c = 1.5 \times 10^{-3} \exp(0.024\rho) \exp(Q/RT)$)

density measurement by pit study was not made continuously with depth (10 cm intervals), it is reasonable that the measured data do not show the seasonal variation like the simulated results. The large density variation observed in the measured data is probably due to other reasons. The variations of initial density and accumulation rate influence the future density. In this paper, to simplify the model, the initial snow density and the accumulation rate are assumed to be constant. However, in reality, the initial snow density accumulated on the surface should change seasonally and the accumulation rate and the snow temperature should change every year. The effect of these factors should be considered in future study.

4. Conclusions

We demonstrated the snow density evolution after deposition, considering that the seasonal variation of snow texture (density, grain size and grain shape etc.) identifying annual layers can be produced by water vapor transportation thorough snow layers and densification due to overburden pressure. It has become clear that the periodic variation of density is due to the influence of water vapor diffusion. The temperature gradient in snow is extremely large for the uppermost 0.2 m. Large snow temperature gradient causes active diffusion of water vapor, thus resulting in the periodic variation

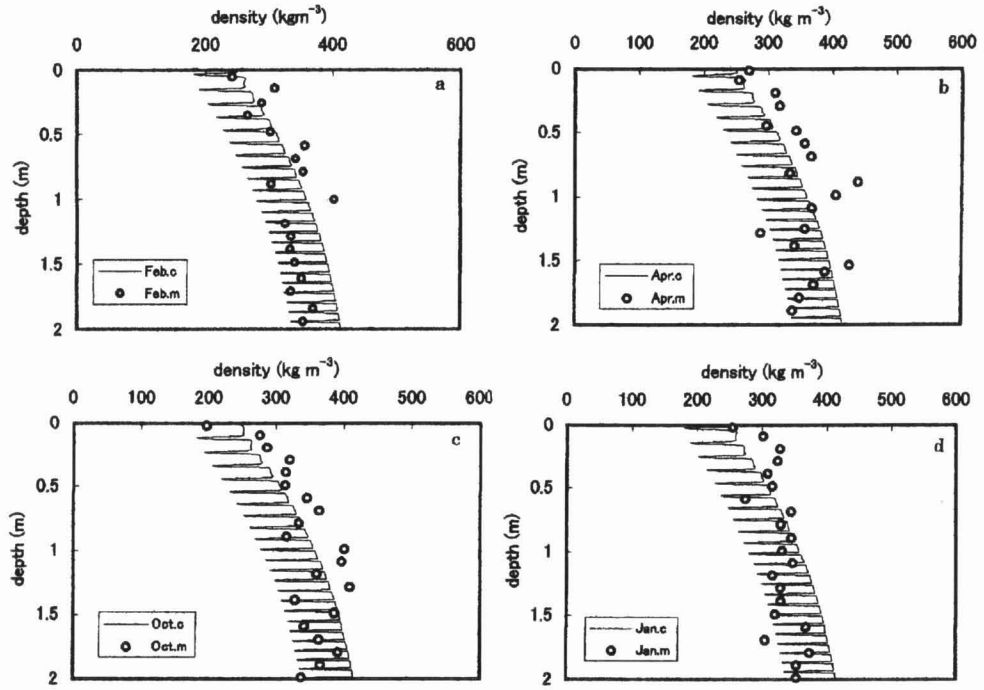

Fig. 9. Comparison of simulated (simulation E(1)) and measured snow density with depth. (a) February. (b) April. (c) October. (d) January. (Solid line is simulated density. Circle is measured density. $\eta_c = 7.5 \times 10^{-3} \exp(0.024\rho) \exp(Q/RT)$ in depth-hoar layer and $\eta_c = 1.5 \times 10^{-3} \exp(0.024\rho) \exp(Q/RT)$ in other snow layers.)

of density with depth. Because water vapor diffuses more actively in summer than in winter, density variation is large in summer layers but is small in winter layers.

It is proved that the accumulation and its seasonal variation influence the density evolution. Smaller accumulation results in larger density variation with depth. And seasonal accumulation influences the variation of annual layers in the density profile. For example, winter type accumulation produces the larger seasonal variation of density than summer type accumulation does.

We also found that the density variation will disappear within the upper one meter owing to densification due to overburden pressure, without a larger compactive viscosity coefficient, for a less dense summer layer

This simulation model should be improved in future study as follows. First, annual variations of snow temperature, accumulation rate and density should be considered in the model. Next, there is need for a model to compute the continuous variation of grain size and shape with depth.

Acknowledgments

We wish to thank Dr. H. Narita of the Institute of Low Temperature Science, Hokkaido University and Dr. Y. Fujii of the National Institute of Polar Research, for

their helpful advice and helpful papers supplied. And we would like to thank Dr. Y. Takeuchi of the Forestry and Forest Products Research Institute and Dr. A. Hachikubo of Kitami Institute of Technology, for their helpful suggestions and encouragement to this study. Finally, we wish to thank two anonymous reviewers for their valuable advice on this paper.

References

Azuma, N., Kameda, T., Nakayama, Y., Tanaka, Y., Yoshimi, H., Furukawa, T. and Ageta, Y. (1997): Glaciological data collected by the 36th Japanese Antarctic Research Expedition during 1995–1996. JARE Data Rep., **223** (Glaciology 26), 83 p.

Brun, E., Martin, E., Simon, V., Gendre, C. and Coleou, C. (1989): An energy and mass model of snow cover suitable for operational avalanche forecasting. J. Glaciol., **35**, 333–342.

Brun, E., David, P., Sudul, M. and Brunot, G. (1992): A numerical model to simulate snow-cover stratigraphy for operational avalanche forecasting. J. Glaciol., **38**, 13–22.

Colbeck, S.C. (1980): Thermodynamics of snow metamorphism due to variations in curvature. J. Glaciol., **26**, 291–301.

Colbeck, S.C. (1993): The vapor diffusion coefficient for snow. Water Resour. Res., **29**, 109–115.

Dang, H., Genthon, C. and Martin, E. (1997): Numerical modeling of snow cover over polar ice sheets. Ann. Glaciol., **25**, 170–176.

Fujii, Y. and Kusunoki, K. (1982): The role of sublimation and condensation in the formation of ice sheet surface at Mizuho Station, Antarctica. J. Geophys. Res., **87**, 4293–4300.

Kojima, K. (1959): The influence of temperature gradient upon the grain texture, setting rate and brittleness of snow. Teion Kagaku, Butsuri-hen (Low Temp. Sci., Ser. A), **18**, 29–46 (in Japanese with English abstract).

Maeno, N. and Ebinuma, T. (1983): Pressure sintering of ice and its implication to the densification of snow at polar glaciers and ice sheets. J. Phys. Chem., **87**, 4103–4110.

Maeno, N. and Kuroda, T. (1986): Seppyô no Kôzô to Bussei (The structure and physical property of snow and ice). (in Japanese). Tokyo, Kokon Shoin, 209 p. (Kiso Seppyô-gaku Kôza, ed. by N. Maeno and M. Fukuda)

Yosida, Z. (1955): Physical studies on deposited snow, I, Thermal properties. Contrib. Inst. Low Temp. Sci., Ser. A, **7**, 19–74.

(Received January 30, 2002; Revised manuscript accepted July 4, 2002)